Edward F. Shultz
Edward G. Cole
Department of Mechanical Engineering,
University of Wisconsin–Madison,
Madison, WI 53706

Christopher B. Smith
Friction Stir Link, Inc.,
Brookfield, WI 53045

Michael R. Zinn
Nicola J. Ferrier
Frank E. Pfefferkorn[1]
e-mail: pfefferk@engr.wisc.edu

Department of Mechanical Engineering,
University of Wisconsin–Madison,
Madison, WI 53706

Effect of Compliance and Travel Angle on Friction Stir Welding With Gaps

This paper presents an investigation of the effects of friction stir weld tool travel angle and machine compliance on joint efficiency of butt welded 5083-H111 aluminum alloy in the presence of joint gaps. Friction stir welds are produced with a CNC mill and an industrial robot at travel angles of 1 deg, 3 deg, and 5 deg with gaps from 0 mm to 2 mm, in 0.5 mm increments. Results indicate that the more rigid mill resulted in higher joint efficiencies than the relatively compliant robot when welding gaps greater than 1 mm with a 3 deg travel angle using our test setup. The results also show that when gaps exceed 1 mm welds made with a travel (tilt) angle of 5 deg are able to generate higher joint efficiencies than welds made with a travel angle of 1 deg and 3 deg. Based on tool geometry and workpiece dimensions, a simple model is presented that is able to estimate the joint efficiency of friction stir welds as a function of gap width, travel angle, and plunge depth. This model can be used as an assistive tool in optimizing weld process parameters and tool design when welding over gaps. Experimental results show that the model is able to estimate the joint efficiency for the test cases presented in this paper. [DOI: 10.1115/1.4001581]

Keywords: friction stir welding, FSW, aluminum, robotic welding, weld gap

1 Introduction

Friction stir welding (FSW) is a relatively new, solid-state welding technology that does not require melting to occur in the workpiece. Instead, the process uses friction and mechanical plastic deformation to heat and soften the material, allowing mechanical deformation mechanisms similar to extrusion and forging to form a strong joint [1,2]. The fact that the melting point is not reached during FSW facilitates the joining of traditionally unweldable alloys and dissimilar alloys. For high quality welds, the process parameters and tool geometry need to be chosen (optimized) for a particular application [3–5]. Figure 1 shows schematics of the typical FSW process and tool along with associated nomenclature to be used throughout this paper. In general, the rotational axis of the tool is not perpendicular to the workpiece, but is tilted in a plane defined by the weld seam normal to the workpiece surface, as shown in Fig. 1(*b*). Referred to as the *travel angle* or *tilt angle*, this is a significant process parameter because it influences the flow patterns of the stir zone, frictional forces, and the heat generated [6]. Past empirical evidence suggest that a travel angle of approximately 2–3 deg is optimal for many aluminum welding applications where variations in part geometry can be expected. In this paper, we explore how gaps along the weld seam affect this assumption.

Friction stir welding has been shown to have several advantages over fusion welding methods such as lower thermal distortion, improved material properties in the weld joint, lower energy input, and a reduced environmental impact [1]. FSW is still a new technology with technical challenges that need to be investigated. Friction stir welding involves large axial forces that must be applied by large machines such as industrial robots. Friction stir welding processes are sensitive to workpiece variations such as disturbances in material tolerances, gaps (Fig. 2), and mismatch. These variations are often compensated for by a skilled welder but are potentially problematic for an automatic FSW system following a predetermined route. The disturbances can be the result of material variation, handling, and improper fixturing or clamping. Material production processes (e.g., extrusion) may produce geometric variations that would be cost prohibitive to eliminate. If at any time a workpiece is damaged, a deformity can be found on the outer surfaces, typically discovered when abutting the plates. Similarly, improper fixturing and clamping occur when a workpiece is either incorrectly seated for welding, or the clamping mechanism failed, such that the axial forces of the tool are large enough to cause the workpiece to shift out of the intended butt welding position. If a gap exists or is produced, the operator would have the option to reject, rework, refixture the workpiece, or simply weld over the gap. In general, welding over the gap would be the least time consuming and most cost effective option because the workpieces would not have to be replaced and/or scrapped. In order for this approach to be practical, strategies must be in place to join the materials while maintaining the highest joint strength possible. Knowledge of what gap sizes can be successfully welded and the process parameters to be used must be developed. For this reason, a study on how travel angle affects the ability to FSW over gaps was performed.

A geometric model is developed and presented in this paper that predicts the joint efficiency: weld tensile strength divided by the parent material tensile strength, assuming that the weld zone has the same properties as the parent material. It does this by predicting the amount of material displaced by the tool shoulder (i.e., theoretical thinning) and assumes that this material fills the gap between the plates. The predicted joint efficiencies compare well with experimental measurement. The model not only suggests adjustments that can be made in the travel angle and plunge depth to compensate for gaps, but also estimates upper limits of the joint efficiency. Given that the gap compensation is not always used in friction stir welding, tight tolerances are required for abutted materials. The model presented in this paper and experimental results suggest that these tolerances can be reevaluated.

[1]Corresponding author.
Contributed by the Manufacturing Engineering Division of ASME for publication in the JOURNAL OF MANUFACTURING SCIENCE AND ENGINEERING. Manuscript received June 9, 2009; final manuscript received March 21, 2010; published online July 23, 2010. Assoc. Editor: Wei Li.

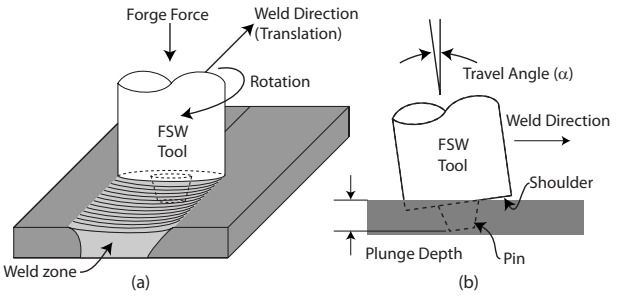

Fig. 1 Schematic of friction stir welding: (*a*) process and (*b*) tool travel angle and plunge depth

2 Related Work

Several research groups have investigated the effects of tool travel angle on friction stir welding. This research has focused on the cause and prevention of weld defects, as well as gap mitigation. Chen et al. [6] studied the effects of tool angle on the generation of weld defects in AA5456, a magnesium solution-hardened alloy. The authors report a critical range of travel angles for minimizing weld defects during friction stir welding, and their effect on the tensile strength of the joint. At travel angles near 1 deg, a surface void is produced on the advancing side of the weld. As the angle is increased to 1.5 deg, the surface void no longer exists, but upon inspection of the cross section, an internal void was generated on the advancing side of the weld. The travel angle is then increased to 3.5 deg and the weld surface is clear of voids with a weld nugget that displays the typical ring pattern. Increasing the angle further to 4.5 deg generated a noticeable increase in forge force in addition to excessive flash on the retreating side and a decrease in weld quality (approximately an 8% reduction in ultimate tensile strength (UTS) and 45% decrease in elongation). The experimental results emphasize the importance of travel angle and its role in depositing materials within the weld.

Van Haver et al. [7] performed a study to assess the weld seam preparation needed for friction stir welding in the event that a gap was unavoidable. They conducted a parametric study (spindle speed, weld speed, plunge depth, and gap width) of FSW of 5 mm thick EN AC-46000-F, a high pressure die cast aluminum alloy. Welds were performed with a 2 deg travel angle with gap widths ranging from 0.2 mm to 1 mm. The authors indicate a reduction in weld zone thickness, weld flaw development, and a significant decrease in tensile strength as the gap increases from 0.2 mm to 1 mm. While internal voids in the weld nugget should not be ignored, Van Haver et al. [7] claimed that the magnitude of flaws or pores in the die cast base material was far more significant than that of the internal voids produced in the weld zone, resulting in the sample failing in the base material when tested despite defects being visible in the weld. Furthermore, an increase in weld pitch (tool revolutions per mm weld length) is shown to be advantageous in welding gaps in friction stir welding, suggesting a relation to heat input. The authors were able to increase the weld quality for gaps of 0.5 mm and 1.0 mm by increasing the plunge depth, but quantitative measurements of the improvement are not available due to the porosity and inclusions present in the parent material. Based on these results, the authors claim that with their weld parameters, gaps of up to 20% (1.0 mm for a 5.0 mm thick plate) can be successfully welded, larger than the 10% figure sometimes used [8].

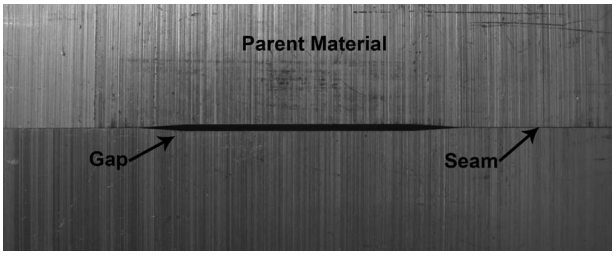

Fig. 2 Photo of a 2.0 mm seam gap between plates to be butt welded

Gap detection was the focus of Yang et al. [9] as they butt welded joints with 3.175 mm thick AA2024 with T3 heat treatment (solution heat treated, cold worked and naturally aged at room temperature). Friction stir welds are produced with a 0 deg travel angle translating perpendicular to the joint gap as opposed to traversing the seam. To analyze the data, the authors use a power spectral density (PSD) of the forge force during the weld, and they find that the $f=0$ Hz (average force) is the best frequency to detect gaps. To detect the gap, a process monitoring algorithm is developed that monitors the moving average of a low pass filtered forge force signal looking for changes in plunge force. Based on the experimental results, a force threshold is determined for the given tool and set of weld parameters. The algorithm is able to detect the presence of the gap before the pin crosses it because the tool shoulder is the first to encounter the gap, giving the operator or controller a chance to make adjustments. Yang et al. [9] stated that this algorithm is not suitable for gaps when the tool travels along the seam of the gap as there is not a sudden change in force to be detected (i.e., what is being studied in this paper).

Gratecap et al. [10] proposed several rules that can be applied to aid in conical FSW tool design and parameter optimization. Of particular interest is a surface area rule where they theorize that the area of the metal displaced by the shoulder should equal the area between the tool and workpiece surface (burr section). If the area of the metal displaced by the shoulder is larger than the burr section, then excess metal will be lost as flash, which does not aid the weld. On the other hand, if the area displaced by the shoulder is not as large as the burr section, then the softened metal stored under the shoulder will decrease in size, reducing the tool-metal interface. This is undesirable because this metal plays a key role in heat generation and conduction.

Despite the research that has been conducted, the best way to deal with gaps during the friction stir welding process is still not known. What gap widths can be welded successfully and when is a gap too large for any set of weld parameters? Previous work indicates that larger tools, travel angles, weld pitches, and tool plunge depths will be beneficial when gaps are encountered. This paper presents a focused study of the effect of travel angle on joint efficiency when welding through different gap widths. A geometric model to predict the optimum travel angle and plunge depth for a given gap size is also presented. The predicted joint efficiency represents an approximation of what is achievable and compares well with experiments.

3 Model

Material flow in friction stir welding is critical to the outcomes of the joining process, including joint strength and the necessary forge force. Both aspects, among others, are also influenced by unexpected disturbances in the weld path such as gaps in abutted plates (Fig. 2). As the tool approaches the gap, the plasticized material is able to escape the weld stir zone and flow into the void created by the gap [9]. When the material escapes, the weld zone no longer maintains the same reactive forces (against the tool) that would typically create the steady state process conditions of the friction stir weld [11]. To overcome the reduction in the material ahead of the tool, due to the gap, a deeper plunge depth or greater travel angle are employed in order to achieve full compaction. However, these can result in a reduced cross section weld (underfill).

To measure these effects, purely geometric calculations are preformed to examine how the tool and workpiece geometry may

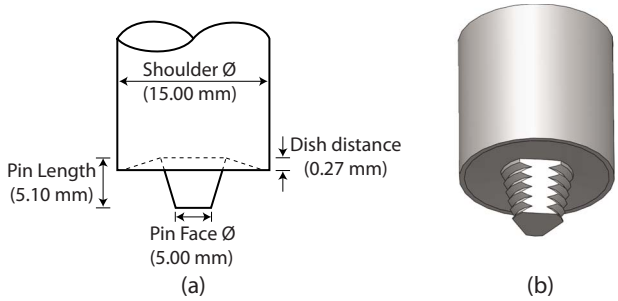

Fig. 3 Schematic of (*a*) key tool dimensions used and (*b*) rendering of tool used

affect maximum theoretical joint efficiency, or the amount of underfill that will be generated. The calculations provide insight that may be useful for tool path design (e.g., travel angle and plunge depth), as well as workpiece tolerance specifications for manufacturing processes.

3.1 Tool Geometry. Friction stir welding tools are developed with various geometries. Tools typically consist of a shoulder and a pin, often with variations in profile features. The tool selected for this study has a shoulder that is slightly concave, and the pin is conical with threads and three flats machined into its surface, similar to the tool shown in Fig. 3. Tool geometry plays a key role when welding. In this paper, the shoulder diameter, travel angle, and plunge depth are used to estimate the material moved by the shoulder, while the pin length, dish distance (shoulder concavity), pin face diameter, and travel angle are used to estimate maximum plunge depths that do not extend beyond the back of the workpiece. The shoulder cavity assists in material retention and heat conduction, the threads help to drive the material to the root of the weld, and the flats serve to locally increase deformation by "paddling" the plasticized material [12,10]. The viscosity and flow of this plasticized material change with material temperature, which is a function of the power input. If the material is either too hot or too cold, the weld will not be ideal [13].

3.2 Weld Strength Assumption. It is known that the refined grain structure of friction stir welds can have a higher tensile strength and ductility than the parent material, especially in slightly work hardened or annealed alloys. Tensile strength of welds made in heat treatable alloys would be expected to be more lose than the parent material. Lacking a comprehensive model to predict these weld material properties, we assume that the weld zone has the same tensile strength as the parent material. This is a significant assumption that may not model the real characteristics of the weld, however, it does provide us with a starting point that allows us to estimate the theoretical joint efficiency based on the thinning of the weld cross section.

3.3 Cross Sectional Analysis. A FSW butt weld viewed down the axis of the weld is represented in Fig. 4. As shown, two abutted plates are joined with the pin center traveling along the faying surfaces of the plates.

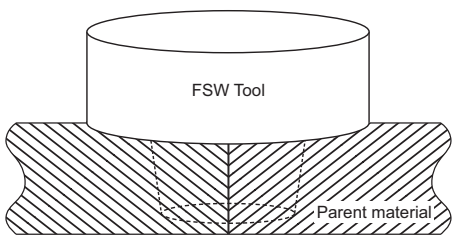

Fig. 4 FSW butt weld as viewed down weld (welding into page)

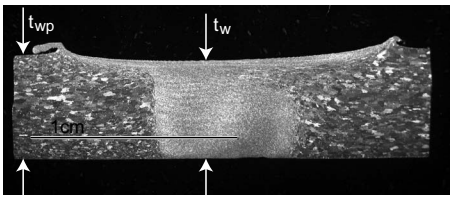

Fig. 5 Weld cross section (AA 5083-H111 etched with modified Poulton's reagent)

3.3.1 Maximum Joint Efficiency. A weld cross section (Fig. 5) will have the thinner section in the middle as a result of the trailing edge of the shoulder traveling below the original workpiece surface (due to the travel angle and plunge depth of the tool). The ridges on the edge of the weld are a combination of the deposited workpiece metal and flash.

Using geometry, and assuming that the elastic deformation is negligible, the thickness at the center of the weld t_W can be found to be the depth of the back of the shoulder subtracted from the thickness of the parent material (Eq. (1)). The thinning of the material in the weld zone is known as the underfill

$$t_W = t_{Wp} - \left[d_{\text{Plunge}} + \frac{\sin(\alpha) \times (\phi_S - \phi_P)}{2} - \cos(\alpha) \times (l_{\text{pin}} - d_D) \right] \tag{1}$$

where t_W is the thinned thickness in the weld zone, t_{Wp} is the parent material thickness, d_{Plunge} is the plunge depth, α is the travel (tilt) angle, $\varnothing_s$ and $\varnothing_p$ are the shoulder and pin diameters, respectively, l_{pin} is the length of the pin, and d_D is the dish distance (Fig. 3). Using only geometry and assuming that the weld material and parent material have the same UTS, an additional equation can then be found that estimates the maximum joint efficiency due to the tool's position

$$J_{ET} = \frac{t_W}{t_{Wp}} \times 100\% \tag{2}$$

Though simple, Eqs. (1) and (2) are powerful because they allow the determination of the maximum allowable travel angle for a specified minimum joint efficiency assuming a full penetration weld. In theory (but not in practice), the travel angle could become so large that for full penetration welds, the shoulder gouges through the entire workpiece thickness. For the tool shown in Fig. 3, the angle where both weld thickness and joint efficiency are zero is determined to be approximately 44 deg.

3.3.2 Plowing. As the FSW tool translates through the workpiece, most of the tool-workpiece contact is from the underside of the shoulder and the pin. Depending on the travel angle and plunge depth, it is possible that the leading edge of the tool shoulder will be below the surface of the workpiece, as shown in Fig. 6.

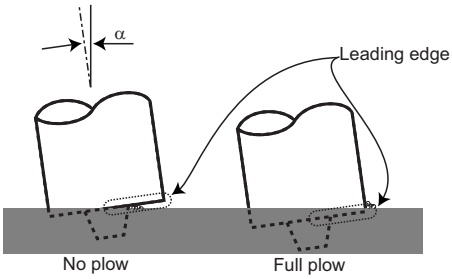

Fig. 6 Plowing as a function of depth

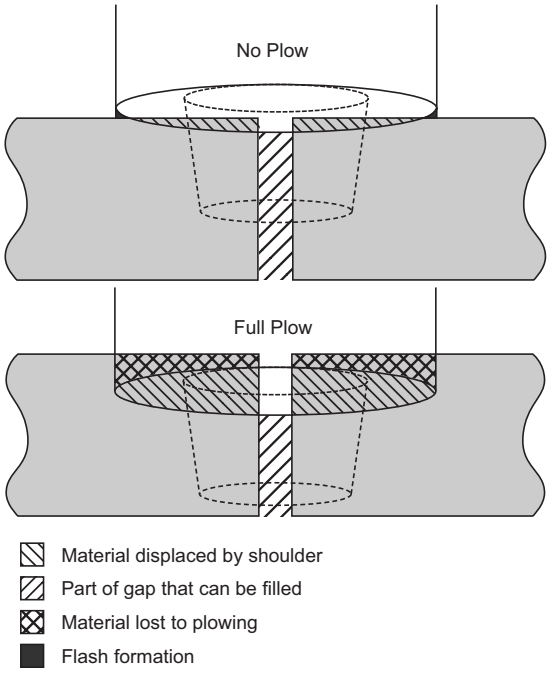

Fig. 7 Weld cross section with a gap showing material lost to plowing, material displaced by the shoulder, and the gap to be filled

This is referred to as "plowing" and it is assumed in the model that any material that contacts the tool between the leading edge and workpiece surface is lost as flash or chips. In other words, this plowed material will not be deposited in the weld or gap. Although plowing may not be ideal, it may be required to achieve the maximum joint efficiency.

3.3.3 Gap Effect. If there is a gap between two abutted plates, then there is an insufficient weld material for maximum joint efficiency. While a weld with zero underfill (and 100% joint efficiency assuming weld strength equivalent to base material) is impossible, it is possible to move the material into the void so that an acceptable weld is formed. This material may come from metal that is displaced by the shoulder in addition to the reserve material under the shoulder. For longer gap lengths, the reserve material would be depleted, so the only available source of material to fill the gap would need to come from the material displaced by the shoulder. For the steady state modeling done in this paper, an infinite gap length is assumed, and thus, stored material under the shoulder is neglected. A simple material flow model assumes that the material under the shoulder fills any gaps below the shoulder, and any excess or plowed material is lost.

During steady state conditions, this problem can be simplified to a 2D area analysis problem, as shown in Fig. 7. The volume per unit length (i.e., area) of the material available to fill the gap A_{Avail} is the difference between the area displaced by the tool shoulder A_d and the area lost to flash A_L

$$A_{\text{Avail}} = A_d - A_L \tag{3}$$

For this paper, all materials shown as plowed in Fig. 7 is assumed to be lost. Additionally, if there was any gap between the tool and workpiece surface, it is assumed that the material is used to form flash there. If the remaining available material is displaced into the gap, then the effective thickness of the filler material in the gap can be written as

$$t_{\text{Gap}} = \frac{A_{\text{Avail}}}{w_{\text{Gap}}} \tag{4}$$

The gap thickness t_{Gap} can then be used to estimate an upper limit to the resulting joint efficiency, assuming that what material does fill the gap is fully compacted

$$J_{EM} = \frac{t_{\text{Gap}}}{t_{Wp}} \times 100\% \tag{5}$$

This can be combined with Eq. (2) to find the maximum predicted joint efficiency based on the assumption of a weld material strength that is equal to the parent material strength

$$J_{EP} = \min(J_{ET}, J_{EM}) \tag{6}$$

Though simple, this model has significant implications for tool design, weld plan selection, and tolerance specifications that will be explored in the following sections.

Table 1 Test matrix

Gap width (mm)	Travel angle (deg)		
	1	3	5
0.00 0.50 1.00 1.50 2.00	Robot	Robot and mill	Robot

4 Experimental Method

To explore the effect of travel angle on the ability to weld over gaps, travel angles of 1 deg, 3 deg, and 5 deg were used to weld 5 mm thick 5083-H111 coupons (Fig. 8) with gap widths of: 0.00 mm, 0.50 mm, 1.00 mm, 1.50 mm, and 2.00 mm machined into them. Welds with a 3 deg travel angle were performed on a CNC mill (Haas TM-1), while welds with 1 deg, 3 deg, and 5 deg travel angles were performed on a robotic FSW system (Friction Stir Link, Inc. Robostir™ system using an ABB IRB 7600 robot). The spindle speed (1500 rpm), weld speed (120 mm/min), tool (Fig. 3), and plunge depth (full penetration) were held constant for all experiments, which were replicated three times (Table 1). All the welds were preformed on a custom built butt weld fixture

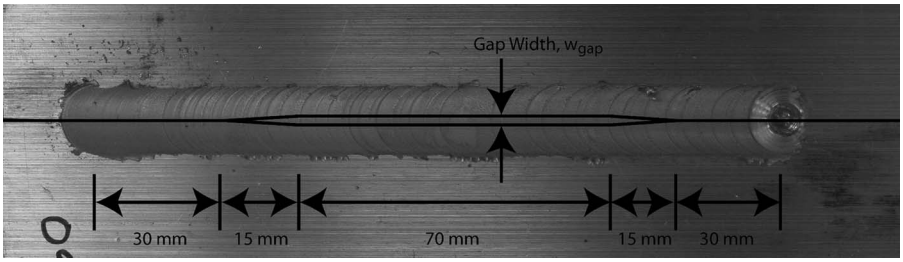

Fig. 8 Photo of weld with 2.00 mm wide gap overlaid

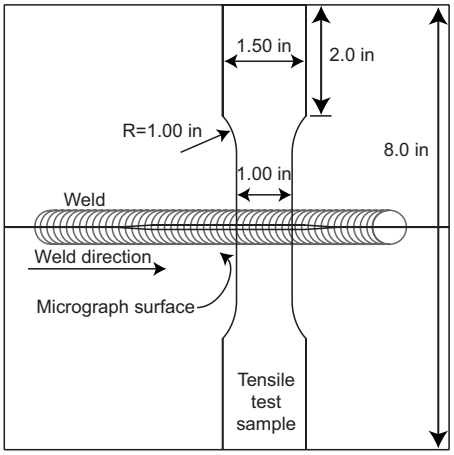

Fig. 9 Location and dimension of tensile test sample

mounted to a three-axis piezoelectric force dynamometer (Kistler 9265B+9443B).

4.1 Industrial FSW Robot. Tests were conducted on a robotic FSW system located at Friction Stir Link, Inc. As shown in Fig. 8, the butt weld begins in an area with nominally zero-gap, transitions into an area with a gap, and then back to the zero-gap weld condition. The transitions are included to help explore the effects of gaps on the forces generated during welding. Nominal weld conditions (given above) that were found to produce an acceptable weld on butt welds of zero-gap were used for all welds.

The ABB industrial robot is designed to accomplish a variety of manufacturing-related tasks. As a result, it has compliance, on the order of 1 mm/kN. This compliance results in large position errors when FSW forces are encountered, which must be compensated for in order to produce the desired joint. For the tests conducted in this study, the forge force was approximately 8 kN, which required the tool location to be commanded 8 mm below the desired position. Although the robot was used in a position control mode, the effect of this offset and the large compliance resulted in a scenario similar to a constant force mode.

4.2 FSW on a CNC Mill. To evaluate the effect of the large compliance of the robot, a similar set of welds was performed on a relatively rigid mill, with an approximate compliance of 0.05 mm/kN. The same gap sizes were welded (Table 1), however, due to hardware limitations, only one travel angle of 3 deg was used.

4.3 Tensile Test and Cross Section Analysis. After the welds were completed, tensile test and macrograph cross section samples were cut from the welded plates (Fig. 9). All welds were tensile tested using AWS B4.0:2007 on a 44 kN (10,000 lbs) test machine (Sintech GL10) with an initial rate of 7.62 mm/min (0.3 in./min). Additionally, a representative cross section from each weld condition was ground, polished, etched, and imaged. The etching was done with a modified Poulton's reagent that had 25 ml of HNO_3 (conc) and 40 ml of 3 g chromic acid per 10 ml of water. Plunge depth measurements were not recorded in situ for either the tests on the robot or mill. Using a custom MATLAB program, the cross section images were analyzed and plunge depths were calculated by fitting a scale outline of the FSW tool to the weld cross sections, as shown in Fig. 10.

5 Results and Discussion

5.1 Comparison of Measured and Predicted Joint Efficiency. The experiment and theoretical calculations provide insight on how travel angle and plunge depth affect joint efficiency. The model is able to predict the joint efficiency reasonably well using only the plunge depth, travel angle, and gap width.

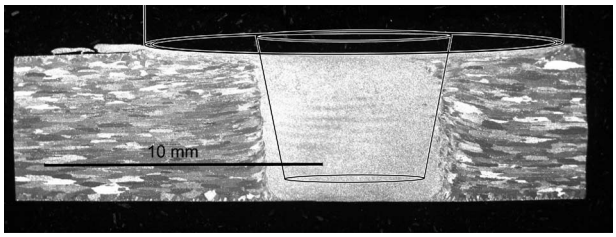

Fig. 10 Macrograph of weld cross section (AA 5083-H111 etched with modified Poulton's reagent) with superimposed tool profile

From Fig. 11, it can be seen that the majority of the model predictions are within 20% of the measured joint efficiencies. It is also seen that the model under predicts the joint efficiency for the mill. It is postulated that this is due to the fact that the mill is better able to push excess materials forward, and thus, is farther from the steady state material flow.

Using the model, it is possible to find optimal values for plunge depth and travel angle for given gap widths. Figure 12 shows these optimal values, as well as the estimated joint efficiencies. Several interesting observations can be made from this plot regarding both the tool design and the operating conditions. For larger gaps, the ideal plunge depth is greater than the workpiece thickness. This would imply that for situations requiring optimal joint efficiencies over larger gaps, a tool with a shorter pin length should be used. The model could be used to aid in tool design, allowing the tool designer to account for joint gaps when specifying tool geometry. The plot also shows that for reasonable gap ranges (<1 mm), a small variation in travel angles can be used, but if the plunge depth is limited, then a much larger range of travel angles is required. For example, for the tool used to generate Fig. 12, a travel angle range of 0–4 deg can optimally friction stir weld gaps up to 2 mm. However, if the plunge is limited to 5 mm (the thickness of the plate), then the optimal travel angle increases to 8 deg for a 2 mm gap.

To help illustrate Fig. 12, only one gap width (2.0 mm) is plotted in Fig. 13, and four (predicted) data points from this graph are plotted in Fig. 14. Figure 13 is effectively a horizontal slice of Fig. 12, and Fig. 14 shows the four predicted points called out in Fig.

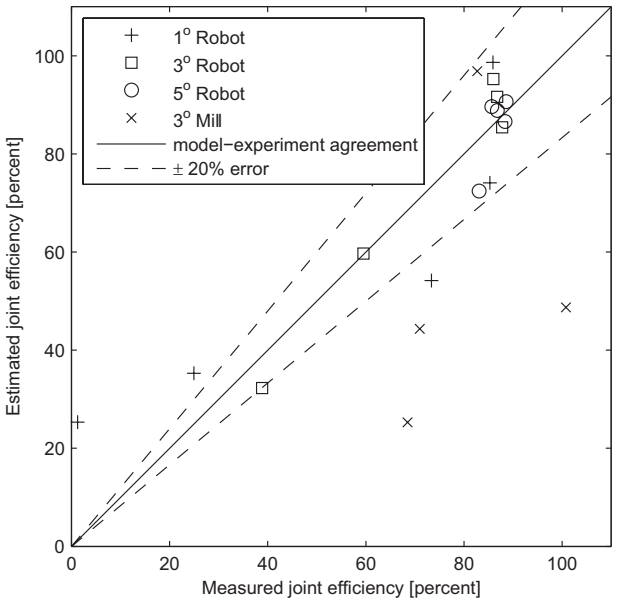

Fig. 11 Comparison of measured and predicted joint efficiency

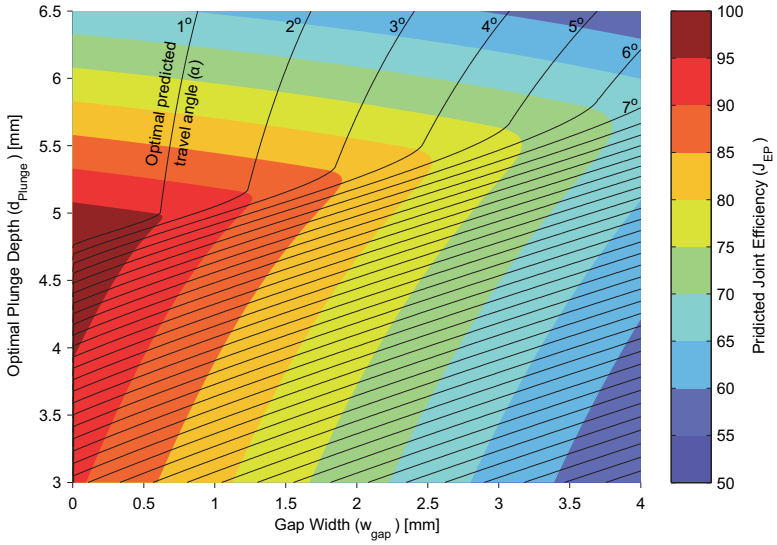

Fig. 12 Predicted travel angle and plunge depth to maximize joint efficiency for a given gap width (5 mm plate, tool design shown in Fig. 3)

13. In both Figs. 12 and 13, one can see that the optimal plunge depth is greater than the 5 mm plate thickness (data point C). This implies that the pin is too long for the tool to weld optimally for a given gap width. However, Fig. 13 shows that when limiting the plunge depth to 5 mm, and increasing the travel angle from 3.9 deg to 7.7 deg (to adjust to the new plunge depth; moving from data point C to B), the predicted joint efficiency only drops from 84.2% to 82.4%. Figure 14 shows several optimal configurations from Fig. 13 for various plunge depths with a 2 mm gap width. Figure 14(*a*) shows the optimal travel angle for a 4 mm plunge depth (data point A). This configuration does not result in the best possible joint efficiency due to the fact that the plunge depth is too shallow, and thus, insufficient material is displaced by the shoulder to fill the gap. Figure 14(*b*) shows a full penetration weld with 5 mm plunge (data point B). This configuration is the best that can be achieved without the pin touching the backing plate. If the pin was shortened, then the shoulder could plunge deeper without the pin contacting the backing plate, allowing for the optimal plunge depth of 5.27 mm, shown as Fig. 14(*c*) (data point C). If the plunge continued deeper, then the joint quality would suffer, as the resulting cross section would be thinner, indicated in Fig. 14(*d*) (data point D). This simple model and corresponding plot would be useful for designers specifying tolerances, as they would be able to estimate joint efficiencies for given gap sizes. This would also be helpful for manufacturers who are trying to optimize FSW where gaps exist.

5.2 Comparison of Robot and Mill. Despite having such large differences in compliance, the industrial robot and the mill produce welds of a similar joint efficiency (~90%) for gap widths up to 1 mm. In this range, the robot produces more consistent results, possibly due to the compliance allowing the robot to react to material variations, whereas the rigid mill is unable. For gaps wider than 1 mm, the welds created by the robot have lower joint efficiencies than those created by the mill. Figure 15 shows a comparison between the robot and mill welds for a 3 deg travel angle over the range of gap widths. The lower performance of the robot on the larger gaps is a result of the tool plunging too deep. The excessive plunging with larger gaps is a result of the large compliance and commanded plunge depth discussed in Sec. 4.1.

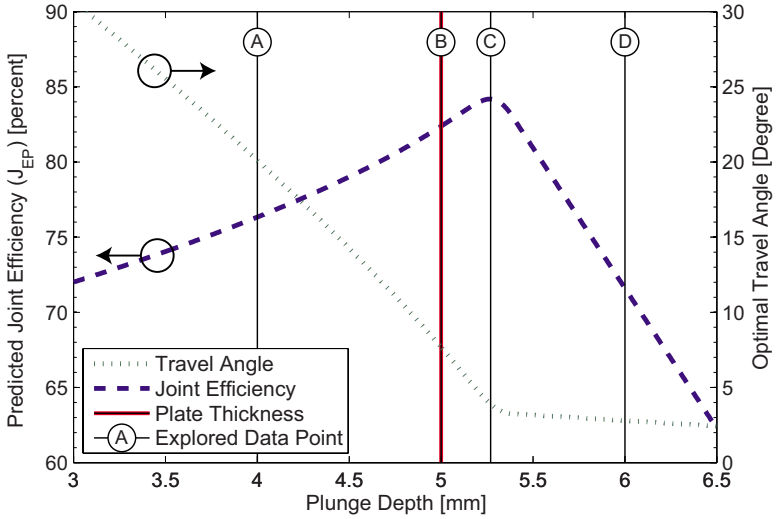

Fig. 13 Predicted maximum joint efficiency and optimal travel angle for various plunge depths for 2 mm wide gap. Data points are shown in Fig. 14.

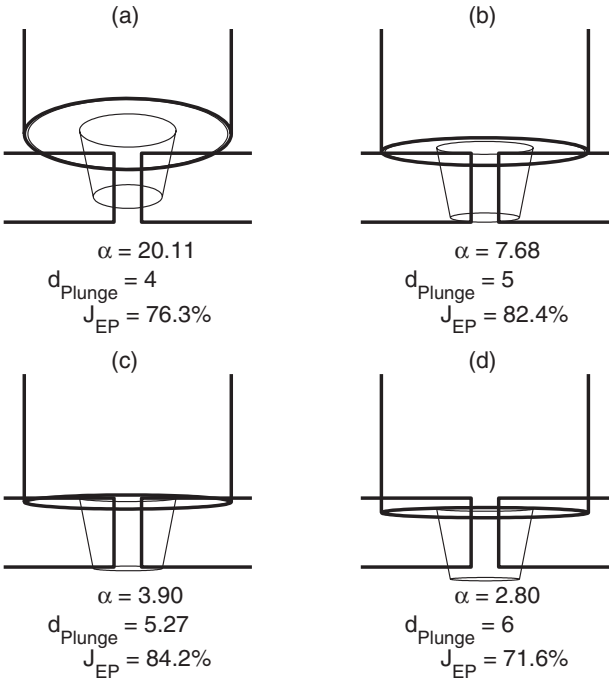

Fig. 14 Optimal angles identified by the model for given plunge depths for a 2 mm gap width. (*a*) 4 mm plunge depth—too shallow for optimal joint efficiency; (*b*) 5 mm plunge depth—maximum plunge without entering backing plate; (*c*) 5.27 optimal plunge depth for joint efficiency as identified by model; (*d*) 6 mm plunge depth too deep.

In areas with larger gaps, the workpiece does not have the necessary material to react the force being applied by the tool, and as a result, it plunges deeper.

Figure 16 shows results from the ABB robot with travel angle variations of 1 deg, 3 deg, and 5 deg. It is immediately noticeable that the 5 deg travel angle maintains a high UTS and joint efficiency over the range of gaps. The consistency of the 5 deg travel angle is far greater than those of the 1 deg and 3 deg travel angles. At 5 deg, a joint efficiency of 85–90% is maintained from zero-gap to 1.5 mm, whereas those of 1 deg and 3 deg decrease rapidly to values below 70% after the 1 mm gap width.

The macrograph cross sections in Fig. 17 provide insight to why the 5 deg travel angle welds are able to perform so well with large gaps and why the 1 deg welds fair so poorly. Despite having a large plunge depth, the 1 deg weld with 2 mm gap (Fig. 17 (c)) lost most of its material due to plowing, and did not have the necessary material under the shoulder to fill in the large gap. The deep plunge observed is a result of the robot's compliance. On the other hand, the shoulder from the 5 deg weld casts a large projection over the potential filler material, and is able to successfully fill in the gap for a relatively strong weld.

6 Conclusions

It has been shown that increasing the travel (tilt) angle for a specified plunge depth reduces the impact of increasing gap widths. However, the maximum attainable joint efficiency decreases with increasing gap width. This is due to the decrease in the weld thickness (increased underfill) as the travel angle increases. Therefore, a gap tolerance can be determined based on the minimum allowable joint efficiency.

Results show that a 5 deg travel angle produces higher joint strength than 1 or 3 deg travel angles when welding across gaps with a robotic FSW system. The robot's compliance results in an increase in the tool's depth as the gap width increases, when operating in position control mode. The robot's compliance can be compensated for by adjusting the vertical offset for known situations, but would require a more complex solution for systems encountering unknown deviations. Increasing the robots rigidity or adding position feedback would be possible solutions to this problem.

A geometric model is developed to predict the thinning for a weld with a steady state gap width, plunge depth, and travel angle. Assuming that the weld has the same ultimate tensile strength as the parent material, the model also predicted the joint efficiency. Even with this assumption, predictions of joint efficiency compare favorably with measured values for 5083 H111 (a nonheat treatable alloy). The model is shown to be a useful tool to maximize joint efficiency for a given gap width by choosing the best combination of travel angle and plunge depth. Additionally, the model can be used to specify gap tolerances if required joint efficiencies are known. The model also shows that the travel angle and plunge depth are strongly related when determining the best tool position and orientation.

Acknowledgment

This work has been partially supported by the Department of Mechanical Engineering, and the College of Engineering at the

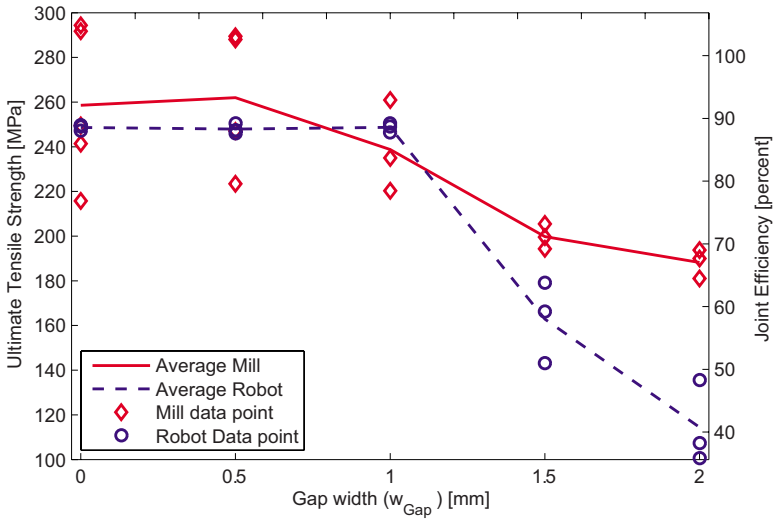

Fig. 15 Comparison of joint efficiency for an industrial robot and CNC mill welding over gaps using a 3 deg travel angle

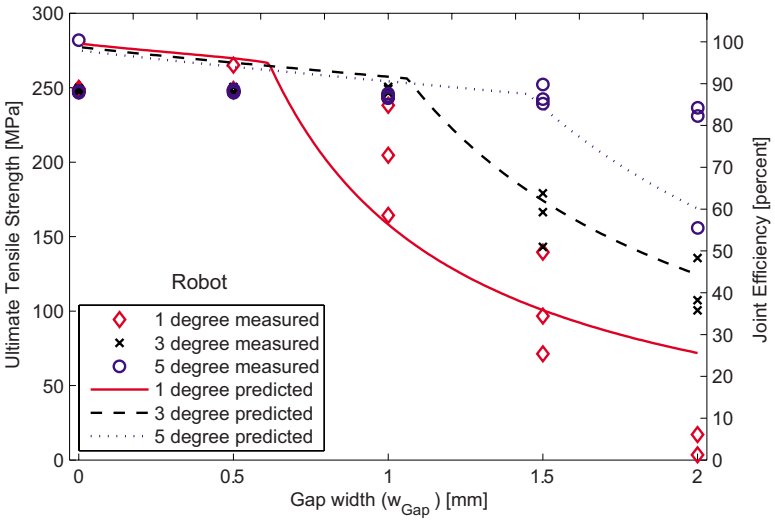

Fig. 16 Effect of travel angle on joint efficiency for various gap widths: measured data for robot welds and predicted values

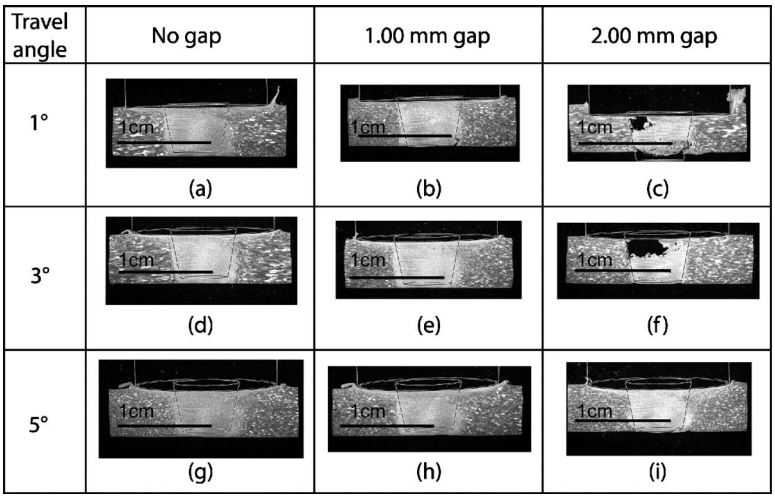

Fig. 17 Micrograph cross sections (AA 5083-H111 etched with modified Poulton's reagent) with tool outline overlaid for robot welds at travel angles of 1 deg (top), 3 deg (middle), and 5 deg (bottom) for gap sizes of 0 mm (left), 1 mm (middle), and 2 mm (right)

University of Wisconsin-Madison, an Industrial and Economic Development Research Grant from the State of Wisconsin, Office of Naval Research STTR Phase I under Contract No. N00014-07-M-0372, and by the National Science Foundation under Grant Nos. CMMI-0824-789 and OCI-0636206. Assistance from the Laser Assisted Multi-Scale Manufacturing Lab has been greatly appreciated. The authors would also like to thank John Hinrichs of Friction Stir Link, Inc. for his advice and discussions on this work.

Nomenclature

α = travel angle (also known as tilt angle) (deg)
$\varnothing_P$ = pin face diameter (m)
$\varnothing_S$ = shoulder diameter (m)
A_d = area (volume/unit length) of material displaced by tool (m^2)
A_L = area (volume/unit length) of material lost to flash and/or plowing (m^2)
A_{Avail} = area (volume/unit length) of material available for gap (m^2)
d_D = dish distance/underfill (m)
d_{Plunge} = plunge depth (m)
J_{EP} = joint efficiency (predicted as resulting thickness÷original thickness) (%)
J_{ET} = joint efficiency limited by tool position (%)
J_{EM} = joint efficiency limited by available material (%)
l_{Pin} = pin length (m)
t_{Gap} = gap material thickness (m)
t_W = reduced weld thickness (m)
t_{Wp} = workpiece thickness (m)
w_{Gap} = gap width (m)

References

[1] Mishra, R., and Ma, Z., 2005, "Friction Stir Welding and Processing," Mater. Sci. Eng. R., **50**(1-2), pp. 1–78.
[2] Thomas, W., Nicholas, E. D., Needham, J. C., Murch, M., Temple-Smith, P., and Dawes, C., 1995, "Improvements Relating to Friction Welding," U.S. Patent No. 061,548,0B1.
[3] Peel, M., Steuwer, A., and Withers, P., 2006, "Dissimilar Friction Stir Welds in AA5083-AA6082. Part II: Process Parameter Effects on Microstructure," Met-

all. Mater. Trans. A, **37**(7), pp. 2195–2206.
[4] Burford, D., Widener, C., and Tweedy, B., Advances in Friction Stir Welding for Aerospace Applications.
[5] 2004, "Exploiting Friction-Stir Welding of Aluminium," *The Naval Architect*, The Royal Institution of Naval Architects, London, p. 11.
[6] Chen, H., Yan, K., Lin, T., Chen, S., Jiang, C., and Zhao, Y., The Investigation of Typical Welding Defects for 5456 Aluminum Alloy Friction Stir Welds.
[7] Van Haver, W., Stassart, X., de Meester, B., and Dhooge, A., Friction Stir Welding of Aluminium High Pressure Die Castings; Parameter Optimization and Gap Bridgeability.
[8] Hatten, T. E., and Arbegast, W. J., 2003 "Apparatus and Method for Friction Stir Welding Using Filler Material," U.S. Patent No. 6,543,671.
[9] Yang, Yu., Kalya, P., Landers, R. G., and Krishnamurthy, K., 2008, "Automatic Gap Detection in Friction Stir Butt Welding Operations," Int. J. Mach. Tools Manuf., **48**, pp. 1161–1169.
[10] Gratecap, F., Racineux, G., and Marya, S., 2008, "A Simple Methodology to Define Conical Tool Geometry and Welding Parameters in Friction Stir Welding," International Journal of Material Forming, **1**(3), pp. 143–158.
[11] Peel, M., Steuwer, A., Withers, P., Dickerson, T., Shi, Q., and Shercliff, H., 2006, "Dissimilar Friction Stir Welds in AA5083-AA6082. Part I: Process Parameter Effects on Thermal History and Weld Properties," Metall. Mater. Trans. A, **37**(7), pp. 2183–2193.
[12] Mishra, R. S., and Mahoney, M. W., 2007, *Friction Stir Welding and Processing*, ASM International, Materials Park, OH.
[13] Reynolds, A. P., 2006, "Aluminium Alloys, Combined Simulation and Experiment for Friction Stir Welding Process Development," *Material Science Forum*, Vol. 519–521, Trans Tech Publications, Ltd., Switzerland, pp. 1095–1100.